Comparison of a thermospheric photochemical model with Student Nitric Oxide Explorer (SNOE) observations of nitric oxide

C. A. Barth
Laboratory for Atmospheric and Space Physics, University of Colorado, Boulder, Colorado, USA

S. M. Bailey
Geophysical Institute, University of Alaska, Fairbanks, Alaska, USA

Received 8 September 2003; revised 8 January 2004; accepted 23 January 2004; published 13 March 2004.

[1] A time-dependent thermospheric model has been used to calculate the nitric oxide density in the lower thermosphere for a 935-day period, 11 March 1998 to 30 September 2000. This model uses daily values of the observed solar soft X-ray irradiance (2–7 nm) as an energy input parameter. The model does not include an energy input from auroral electron precipitation. The results of the model calculation of nitric oxide density at 110 km were compared with observations of nitric oxide density made with the Student Nitric Oxide Explorer (SNOE) for the 935-day period. At the equator the model calculations and the observations agree very well with a linear correlation coefficient of 0.876. The correlation coefficient remains high for the altitude region 107–117 km, the region where solar soft X-rays (2–7 nm) are the major source of nitric oxide production. The comparison of the model calculations with the observations as a function of latitude show that there is excess nitric oxide poleward of 30°N and S latitude particularly during the fall-winter season. We believe that the source of this excess nitric oxide is the nitric oxide that is produced in the auroral region (65°–75°N and S geomagnetic latitude) by precipitating auroral electrons. We believe that aurorally produced nitric oxide is transported equatorward by horizontal winds. At midlatitudes the excess nitric oxide decays to about half of its initial value in one day. At times of large geomagnetic storms we believe that aurorally produced nitric oxide is transported all the way to the equator by horizontal winds. The excellent correlation of the model calculations and the SNOE observations of nitric oxide at 110 km between 30°S and 30°N support the hypothesis that solar soft X-rays are the source of the variability of nitric oxide in the thermosphere at low latitudes. *INDEX TERMS:* 0355 Atmospheric Composition and Structure: Thermosphere—composition and chemistry; 0358 Atmospheric Composition and Structure: Thermosphere—energy deposition; 0310 Atmospheric Composition and Structure: Airglow and aurora; 2704 Magnetospheric Physics: Auroral phenomena (2407); 2716 Magnetospheric Physics: Energetic particles, precipitating; *KEYWORDS:* nitric oxide, nitric oxide model, SNOE observations

Citation: Barth, C. A., and S. M. Bailey (2004), Comparison of a thermospheric photochemical model with Student Nitric Oxide Explorer (SNOE) observations of nitric oxide, *J. Geophys. Res.*, *109*, A03304, doi:10.1029/2003JA010227.

1. Introduction

[2] Global observations of nitric oxide in the lower thermosphere have been made for a period of 935 days during the ascending portion of the solar cycle, 11 March 1998 and 30 September 2000 [*Barth et al.*, 2003]. The density of nitric oxide whose maximum in altitude occurs near 110 km is highly variable as a function of latitude and of time. There are two principal energy sources that lead to the production of nitric oxide that are highly variable, solar soft X-rays and auroral electron precipitation [*Barth*, 1992]. The solar soft X-ray irradiance has also been measured during this period from the same satellite that makes the nitric oxide observations, namely, the Student Nitric Oxide Explorer (SNOE) [*Bailey et al.*, 2000]. The flux of precipitating electrons has been measured by a number of satellites [*Baker et al.*, 2001]. In addition to the variable energy sources, the distribution of nitric oxide in the thermosphere is affected by atmospheric motions, both vertical and horizontal.

[3] The calculation of the production of nitric oxide from the solar soft X-rays is particularly challenging. In interacting with the atmospheric constituents, the solar X-rays in the 2–7 nm wavelength region produce photoelectrons. These photoelectrons produce additional ionization, which in turn produces excited nitrogen atoms. These excited nitrogen atoms produce nitric oxide when they react with molecular oxygen. Nitric oxide is destroyed by solar far ultraviolet radiation. The differing optical depths of the solar

0148-0227/04/2003JA010227$09.00

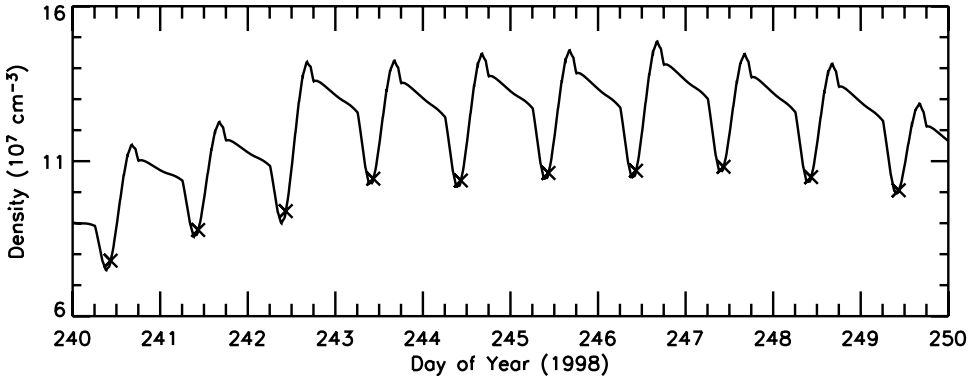

Figure 1. Model calculation of nitric oxide density for a 10-day period starting on day 240 of 1998. The density is calculated every 5 min. This plot shows the diurnal variations. The crosses indicate the time when the model calculation corresponds to the observations.

soft X-rays and solar far ultraviolet radiation leads to a varying density of nitric oxide as a function of solar zenith angle. The nitric oxide density changes as a function of the time of day and the latitude. The solar soft X-rays vary by about a factor of two during the 27-day rotation period of the sun and by another factor of two during the 2 1/2 years of the increasing solar cycle [*Bailey et al.*, 2000]. The time-dependent, photochemical model that is used in this paper is described in detail by *Bailey et al.* [2002].

[4] Earlier model studies [*Siskind et al.*, 1990; *Fuller-Rowell*, 1993; *Siskind et al.*, 1995] determined the range of solar soft X-ray fluxes that were needed to match the nitric oxide densities measured from rocket and satellite measurements. When the solar soft X-ray source of nitric oxide was proposed [*Barth et al.*, 1988], there were no solar X-ray measurements that were made simultaneous with the rocket and satellite nitric oxide observations. In this paper we use solar soft X-ray and nitric oxide measurements that were made simultaneously from the same satellite.

[5] The objective of this paper is to test this thermospheric photochemical model with the SNOE observational dataset. We use the model with only the solar soft X-rays and the solar extreme ultraviolet radiation as energy inputs. We wish to determine what is the latitude range where the solar soft X-rays control the variability of the nitric oxide. We expect that electron precipitation in the auroral region, 65°–75° geomagnetic latitude, controls the nitric oxide density in that latitude region. We wish to learn what influence the nitric oxide produced by auroral electron precipitation may have on the nitric oxide density at low latitudes. We then wish to identify what other processes may be affecting the density distribution of nitric oxide.

2. Nitric Oxide Model

[6] The time-dependent thermospheric model takes into account 35 chemical and ionic reactions and calculates the density of three odd nitrogen species (NO, N(^{2}D), N(^{4}S)) and four ions (N_2^+, O_2^+, O^+, NO^+) [*Bailey et al.*, 2002]. The model atmosphere that is used for the neutral species and the temperature is the NRLMSISE-00 model with inputs of 10.7 cm solar radio flux and Ap geomagnetic index [*Picone et al.*, 2002]. A recent study of observations of nitric oxide in the thermosphere using the ISAAC (Ionospheric Spectroscopy and Atmospheric Chemistry) satellite instrument showed that improved agreement with a photochemical model was obtained using the NRLMSISE-00 model rather than the MSIS90 model [*Minschwaner et al.*, 2004]. The extreme ultraviolet solar flux between 20 and 103 nm is calculated using the model of *Hinteregger et al.* [1981], which uses the solar 10.7 cm flux as an input parameter. The solar soft X-ray irradiance, 2–20 nm, is measured directly from the SNOE spacecraft [*Bailey et al.*, 2000]. The photoelectron fluxes are calculated using the glow model of *Solomon et al.* [1988]. In this one-dimensional thermospheric model, vertical transport by molecular and eddy diffusion is taken into account using the formalism of *Colegrove et al.* [1965]. An eddy diffusion coefficient of 1×10^{-6} cm^2 s^{-1} above 100 km is used in these calculations.

[7] For comparison to SNOE observations of nitric oxide density, the model was run for 935 days between 11 March 1998 and 30 September 2000. The model calculations were performed at altitudes between 40 and 250 km at altitude intervals of 2 km and for latitudes between 80°S and 80°N at latitude intervals of 5°. Photoelectron fluxes were calculated 24 times per day at 1-hour intervals using daily solar inputs and then placed onto a 5-min grid. The odd nitrogen and ionic species were calculated with an integration period of five minutes for the 935 days for a total of one-quarter of a million calculations for each latitude. The results at each altitude were interpolated onto a 3.33 km grid for comparison with SNOE observations of nitric oxide density.

[8] An example of the results of the time-dependent calculation is shown in Figure 1. The nitric oxide density at 110 km is calculated at the equator for a 10-day period starting on day 240 of 1998. Following sunrise, the nitric oxide density initially decreases because of photodissociation produced by solar far ultraviolet radiation. The density then increases when solar X-rays illuminate the 110 km level of the thermosphere. Following sunset, the nitric oxide density decreases throughout the night because of transport out of the source region. The SNOE observations were made at a mean local time that was 10:17 AM at the beginning of the 935-day period and slowly changed to 11:11 AM at the end of this period. In comparing model results to SNOE observations, the changing mean solar time was taken into account. The crosses on the figure indicate

the time when the model calculation corresponds to the observation.

3. Nitric Oxide Data

[9] The nitric oxide observations have been described by *Barth et al.* [2003]. These observations were made between 11 March 1998 and 30 September 2000, which was a period of increasing solar activity. At the beginning of the period, the 81-day average of the 10.7 cm radio flux was 100 and at the end of the period, it was 200. The nitric oxide observations were made with a limb-viewing ultraviolet spectrometer which measured the emission from the nitric oxide (0,1) gamma band at 237 nm.

[10] The column emission rate of the nitric oxide gamma band is related to the column density of nitric oxide by the g-factor [*Chamberlain*, 1961, pp. 424–425]. The g-factor or photon scattering coefficient is made up of the oscillator strength of the absorption band, the branching ratio of the emission band, and the solar flux plus a combination of physical constants. The oscillator strength and the branching ratios are determined from laboratory measurements. The solar flux is measured by ultraviolet spectrometers on space vehicles. For molecular airglow emissions such as the gamma bands, it is very important to have high-resolution spectra because of strong absorption lines in solar spectrum [*Chamberlain*, 1961, pp. 438–444].

[11] Several calculations of the g-factors of the nitric oxide gamma bands have been made. A high-resolution (0.1 nm) solar spectrum obtained on 3 August 1985 from the Spacelab 2 Shuttle Solar Ultraviolet Spectral Irradiance Monitor (SUSIM) [*VanHoosier et al.*, 1988] was used to calculate g-factors for the analysis of rocket measurements of the nitric oxide day airglow [*Eparvier and Barth*, 1992]. These calculations gave values of 6.37×10^{-6} and 2.25×10^{-6} photons/sec-molecule at 280K for the (1,0) and (0,1) gamma bands. *Stevens* [1995] used a higher-resolution (0.01 nm) solar spectrum from a balloon-borne experiment [*Hall and Anderson*, 1991] to calculate g-factors. This spectrum was normalized to measurements made by the moderate resolution (1 nm) Solar-Stellar Irradiance Comparison Experiment (SOLSTICE) [*Rottman et al.*, 1993] for observations made on 25 February 1992. The Stevens calculations gave values of 6.77×10^{-6} and 2.63×10^{-6} photons/sec-molecule at 200 K for the (1,0) and (0,1) gamma bands. The SOLSTICE measurements which were made from the Upper Atmosphere Research Satellite (UARS) have produced a 10-year long database which includes the time of the 25 February 1992 calculation and the period of the SNOE observations, 11 March 1998 through 30 September 2000. The UARS SOLSTICE observations have been compared to observations made by UARS SUSIM, ATLAS SUSIM, and ATLAS SSBUV on March 29, 1992 [*Woods et al.*, 1996]. The ATLAS missions are shuttle Atmospheric Laboratory for Applications and Science (ATLAS) missions. For the wavelength region that includes the nitric oxide bands, all four instruments agreed to within 7%.

[12] We compared the Spacelab 2 SUSIM solar flux at 226 nm with the SOLSTICE solar flux at that wavelength for the same day. The SUSIM value is about 10% low compared with the SOLSTICE value. Since SOLSTICE has a long-term database that has been repeatedly compared to a set of standard stars, we are using the SOLSTICE data as the standard monitor of the magnitude of the solar flux. For comparison with the SNOE observations of nitric oxide over a 935-day period, the SOLSTICE database is used to obtain the daily variation of solar flux at 226 nm. Since the *Stevens* [1995] calculation has the most extensive calculation of the nitric oxide rotational structure together with the *Hall and Anderson* [1991] high-resolution solar spectrum, we have adopted the *Stevens* [1995] g-factors as normalized to SOLSTICE on 25 February 1992. Table 1 shows the g-factors for the (0,1) gamma band as a function of temperature.

Table 1. (0,1) Nitric Oxide Gamma Band g-Factors

K	10^{-6} Photons/Sec-Molecule
200	2.63
300	2.60
400	2.61
500	2.64
600	2.66
700	2.69
800	2.71
900	2.72
1000	2.73
1100	2.74
1200	2.74

[13] Since the analysis of SNOE nitric oxide observations in this paper emphasizes the 110 km region where the temperature lies in the range 230–260 K, we use a value of 2.62×10^{-6} for the 25 February 1992 standard calculation and we use the SOLSTICE solar flux at 226 nm to calculate the daily value of the (0,1) g-factor to determine the nitric oxide density from the SNOE observations. In the paper describing the SNOE database [*Barth et al.*, 2003], we used a value of 2.25×10^{-6} for the (0,1) g-factor, a value that is 14% less than the value used here. The magnitude of the SUSIM solar flux at 226 nm accounts for 10% of that difference and the more complete calculation of the rotational structure [*Stevens*, 1995] accounts for 4% of the difference. The ratio between the *Eparvier and Barth* [1992] g-factor and the value used in this analysis is 0.856.

[14] For the 935-day period of the nitric oxide dataset, the largest variation of the g-factor comes from the $1/r^2$ dependence of the solar flux produced by the varying heliocentric distance of the Earth. In addition, the daily variation of the solar flux at 226 nm, which is measured by SOLSTICE, is taken into account. Figure 2 shows the magnitude of the g-factor for the 935-day period from 11 March 1998 to 30 September 2000.

4. Comparison of Model With Observations at the Equator

[15] The initial comparison of the model with observations was done at the equator (2.5°S to 2.5°N). Daily nitric oxide densities were averaged for a 19-day period centered on 20 March 1998, the spring equinox. These observations were compared with the model calculation for the equator for 20 March 1998 (day of year 79) over the altitude range 93–130 km and plotted in Figure 3. The apparent agreement in magnitude is excellent considering that the uncertainty in the instrument calibration is about 14% [*Barth et*

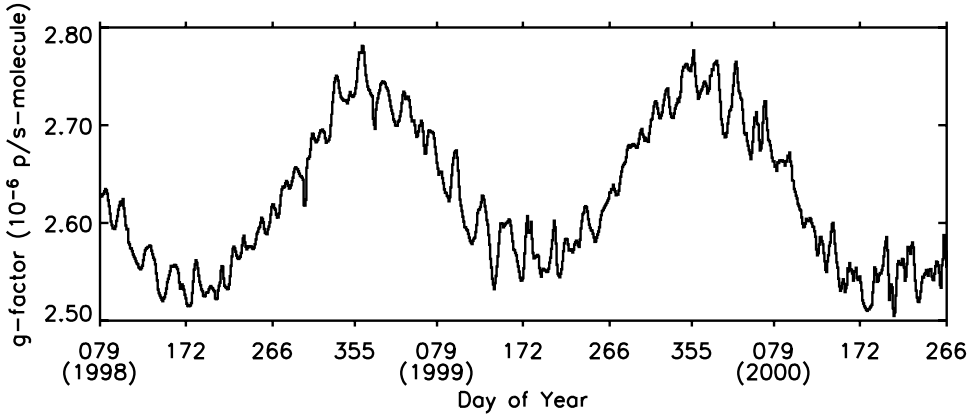

Figure 2. Value of the (0,1) nitric oxide gamma band g-factor for the 935-day period of SNOE observations. The variations due to the changing heliocentric distance and solar activity are shown.

al., 2003], the uncertainty in the solar flux used to calculate the g-factor is about 7% [*Woods et al.*, 1996], and the uncertainty in the molecular parameters used to calculate the g-factor is about 10% [*Barth*, 1992]. The model calculation also has a number of uncertainties. Any systematic error in the NRLMSISE-00 model will produce a proportional error in the nitric oxide model calculation. The sum of the uncertainties in key reaction rates in the model is estimated to be 20%. The energy input into the model, the solar soft X-ray irradiance has an uncertainty of 10%. The counting statistics for the nitric oxide densities in Figure 3 is less than 2%. For all these reasons, the apparent excellent agreement between model and observations should not be overinterpreted.

[16] A more stringent test of the model is the comparison of the time variation of the daily values of nitric oxide at a fixed altitude with the model calculation at the same time of the day. A comparison of the daily variation of nitric oxide density from observations and from model calculations is shown in Figure 4 for an altitude of 110 km at the equator for the 935-day period. The statistical uncertainty in the daily averages of the nitric oxide densities is 5%. The 27-day time variation of the model follows the observations very well. The long-term variation is also satisfactory with a hint of a seasonal variation in the ratio of the observations to the model. During this period of increasing solar activity, the 81-day mean of the nitric oxide density at the equator increased from 5×10^7 molecules cm^{-3} at the beginning of the period to 1×10^8 molecules cm^{-3} at the end of the period.

[17] The correlation of the two 935-day sets, the observations and the model calculations, was calculated. At 110 km, the linear correlation coefficient of the observation model comparison was 0.876 for 568 days of the 935-day period when auroral activity was low (Ap less than 12). Figure 5 shows a scatter plot of nitric oxide density as calculated from the model and as observed from SNOE. A linear least-squares fit was performed on these data sets that took into account that both data sets vary independently. The slope was determined to be 1.046 and the intercept 3×10^4 molecules cm^{-3}. A solid line with this slope and intercept is plotted on the figure.

[18] The correlation coefficients of the 935-day time series for the model and observations were calculated as a function of altitude. The results are listed in Table 2 together with the ratio of the mean observation densities to the mean model densities.

[19] An inspection of the table shows that the linear correlation coefficient has the largest values in the 107–117 km altitude region. This is the region where the production of nitric oxide is greatest [*Bailey et al.*, 2002]. The variation in the ratio of the observations to the model density as a function of altitude indicates that the model still has shortcomings. For example, the use of future observations of the solar soft X-ray flux at higher resolution than was obtainable with the SNOE instrument may lead to a different altitude variation of photoelectron production than is calculated in the current model. Another uncertainty may have to do with the NRLMSIS molecular oxygen densities that are used in the model calculations particularly above 120 km. Uncertainties below 120 km may have to do with the eddy diffusion coefficient that was used in the calculations.

5. Comparison of Model With Observations at All Latitudes

[20] The model calculation of nitric oxide density at 110 km is plotted for all latitudes in Figure 6 (top). This calculation used inputs from only solar soft X-rays and

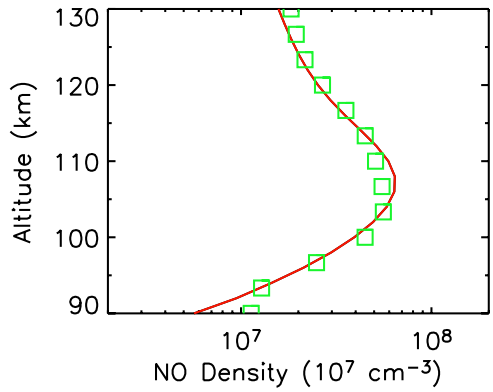

Figure 3. Model calculations (red line) and SNOE observations (green squares) of the altitude variation of nitric oxide density for the spring equinox (1998) at the equator.

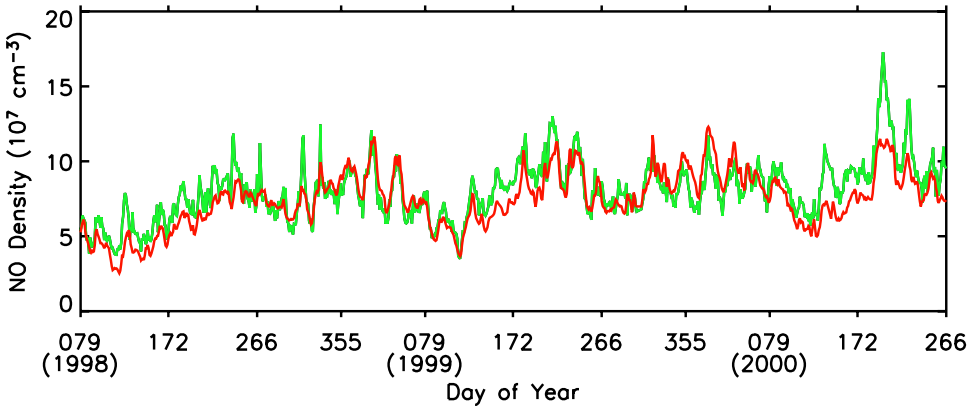

Figure 4. Comparison of model calculations (red line) and SNOE observations (green line) of the nitric oxide density at 110 km at the equator.

extreme ultraviolet radiation without any input from auroral electron precipitation. Most apparent is the seasonal effect. The location of the maximum density as a function of latitude moves northward and southward with the seasons with the maximum nitric oxide density occurring in the spring-summer hemisphere. Only at the equinoxes is the maximum nitric oxide density near the equator. The model clearly shows the 27-day variation of nitric oxide density produced by the 27-day variation in the solar soft X-ray irradiance. The model also shows the long-term increase in nitric oxide density as a result of increasing solar activity during the ascending phase of the solar cycle.

[21] The observations of nitric oxide density at 110 km as a function of latitude are plotted in Figure 6 (middle) [*Barth et al.*, 2003]. This dataset uses the g-factors plotted in Figure 2, which include the variation produced by the varying heliocentric distance of the Sun and the changing solar ultraviolet irradiance. A comparison with the model shows many of the same seasonal and 27-day variations as the model. The observations, however, include the nitric oxide produced in the auroral region from electron precipitation [see *Baker et al.*, 2001; *Barth et al.*, 2003]. The model calculation does not include the effects of the precipitation of auroral electrons into the atmosphere.

[22] To see the effects of the auroral energy input, we subtracted the nitric oxide densities calculated with the model from the observed nitric oxide densities. The residuals are shown in Figure 6 (bottom). (Negative values have been set equal to zero in this figure.) There is substantial excess nitric oxide at high latitudes particularly in the fall-winter hemispheres. Auroral electron precipitation occurs in the latitude band 65°–75° geomagnetic latitude [*Newell et al.*, 1996]. Since the nitric oxide densities in Figure 6 are daily averages plotted in geographic coordinates, nitric oxide resulting from electron precipitation is spread out over geographic latitudes 55°–85°. Figure 6 (bottom) shows that there is substantial excess nitric oxide equatorward of 55°. We believe that this nitric oxide has been transported equatorward by horizontal winds. This figure also shows that there are a number of occasions where it appears that nitric oxide has been transported all the way to the equator.

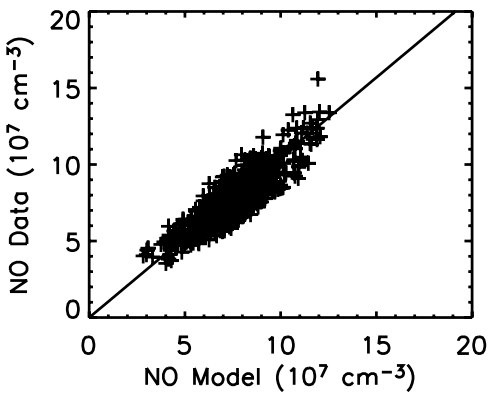

Figure 5. Correlation of model calculations and SNOE observations of nitric oxide density at 110 km. Crosses show the model-observation values for a 568 day period (out of 935) when the auroral activity was low (Ap < 12). The solid line is a least-squares fit of the observations to the model.

6. Discussion

[23] Nitric oxide is produced in the thermosphere through a series of chemical and ionic reactions that are initiated by solar X-ray photoelectrons and by auroral electrons. Nitric oxide is destroyed by a number of processes some of which recycle the nitric oxide back into other forms of odd

Table 2. Correlation of Model Densities and Observation Densities[a]

Altitude, km	Coefficient	Ratio
130	0.748	1.46
127	0.733	1.47
123	0.751	1.51
120	0.782	1.53
117	0.835	1.46
113	0.868	1.27
110	0.844	1.03
107	0.830	0.90
103	0.772	0.92
100	0.603	0.95
97	0.375	0.84

[a]Ratio of the mean observation density to the mean model density.

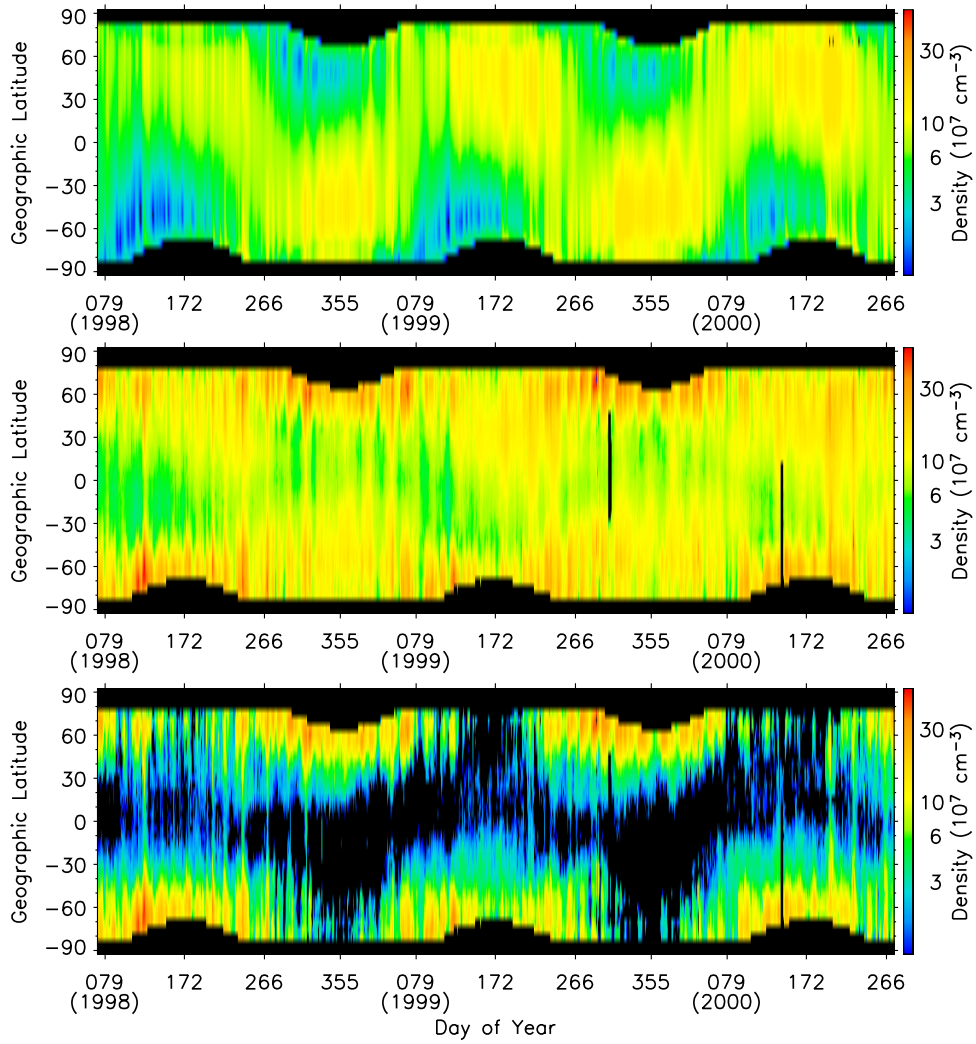

Figure 6. Comparison of model calculations and SNOE observations as a function of latitude at 110 km. (top) Model calculations. (middle) SNOE observations. (bottom) Residuals from subtraction of model calculations from SNOE observations. (Negative values of the residuals have been set equal to zero.)

nitrogen. The one loss process that changes nitric oxide into molecular nitrogen is the photodissociation of nitric oxide by solar far ultraviolet radiation followed by the reaction of ground state atomic nitrogen with nitric oxide. The effective lifetime of this process is 19.6 hours [*Minschwaner and Siskind*, 1993; *Murray et al.*, 1994; *Siskind*, 2000]. While formally this lifetime applies to nitric oxide that is being illuminated by solar ultraviolet radiation when there are no

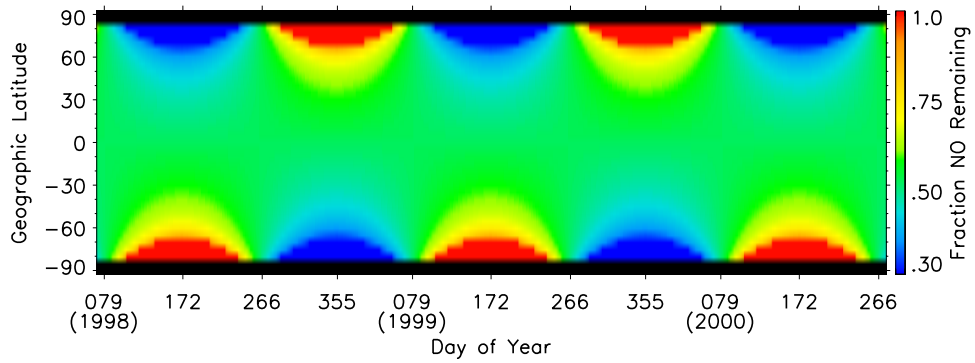

Figure 7. Fraction of nitric oxide remaining after 1 day. At the equator, any excess nitric oxide decreases to about 50% of its initial value after 1 day.

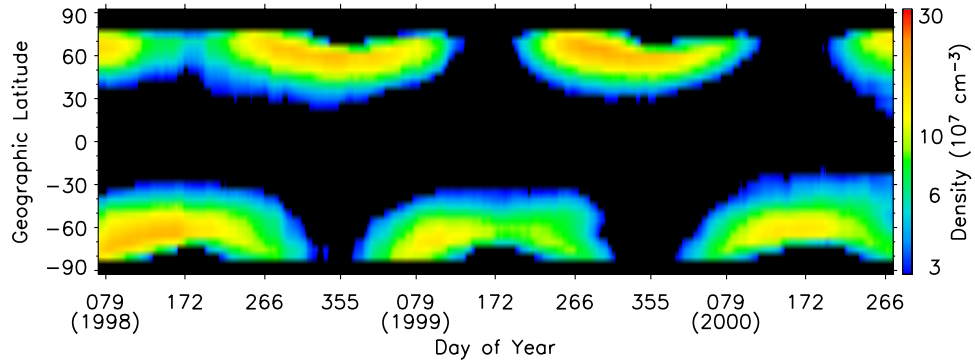

Figure 8. Seasonal distribution of excess nitric oxide. The residuals from the subtraction of smoothed model from smoothed observations are plotted. Compared to Figure 6 (bottom), the lower limit of the color scale has been changed.

processes producing nitric oxide, this lifetime also applies to any excess nitric oxide that is present when nitric oxide is in equilibrium with production and loss mechanisms. This applies to the situation where excess nitric oxide is transported out of the auroral region to low latitudes where the density of nitric oxide is controlled by solar soft X-rays and solar ultraviolet radiation. For example, at the equator at equinox when the length of daylight is 12 hours, the amount of excess nitric oxide decreases to 54% of its initial value during a 24-hour period. The fraction of nitric oxide remaining after 1 day has been calculated for all latitudes and all seasons for the 935-day period and is displayed in Figure 7. During polar night when there is no solar ultraviolet radiation, nitric oxide is not destroyed and the fraction remaining is 100%. During polar summer when there is 24 hours of illumination, the fraction of nitric oxide remaining is 29%. A comparison of Figure 7 with Figure 6 may be used to understand how long excess nitric oxide that may be transported from the winter polar region to the equator would exist. It would decrease to about 50% of its initial density in one day. Any remaining excess nitric oxide would decay by a factor of two each day until it reach the value appropriate to the illumination of the equatorial region by solar soft X-rays.

[24] To further explore the distribution of excess nitric oxide that has been transported equatorward from the auroral region, we smoothed the model calculations and the observations shown in Figure 6 with a 91-day moving average. We subtracted the smoothed model calculations from the smoothed observations and plotted the results in Figure 8. This figure clearly shows that there is aurorally produced nitric oxide at midlatitudes in the fall-winter seasons. This excess extends equatorward to about 30° latitude. The maximum in the excess nitric oxide actually appears during the fall season. We believe that this distribution is the result of atmospheric transport out of the auroral region toward the equator during the fall-winter season. Using Figure 8 as a guide, we calculated the linear correlation coefficient between model calculations and observations at 110 km as a function of latitude. Between 30°S and 30°N, the correlation coefficient was greater than 0.8. Poleward of those latitudes, the correlation coefficient decreased to smaller values reaching values less than 0.5 poleward of 45°N and S latitude. The conclusion is that the thermospheric model using only solar soft X-rays and extreme ultraviolet radiation as energy inputs adequately describes thermospheric nitric oxide at the 110 km level between 30°S and 30°N. Poleward of that region, the model needs to include electron precipitation in the auroral region and atmospheric transport out of the auroral region.

[25] We showed earlier [*Baker et al.*, 2001] that nitric oxide in the auroral electron precipitation region (60°–70° north and south geomagnetic latitude) was correlated with satellite measurements of precipitating electrons. A comparison of measurements of the hemispheric power index from the Polar Orbiting Environmental Satellites (POES) with SNOE nitric oxide density measurements showed a correlation coefficient of approximately 0.63. We interpret that result as evidence that precipitating electrons are producing nitric oxide in the auroral region. In this paper we interpret the excess nitric oxide at 60°N and S geographic latitude as having been produced by auroral precipitating electrons. We interpret the excess nitric oxide equatorward of 60°N and S latitude as having been transported there by atmospheric motions. In Table 3 we have listed the results of correlating the excess nitric oxide at latitudes between 30°N and S and 55°N and S with the excess nitric oxide at 60°N and S. The coherence of the time variation of the nitric oxide distribution gradually diminishes in moving away from the source region. We interpret this pattern as evidence of atmospheric transport equatorward from the auroral region.

Table 3. Correlation of Excess Nitric Oxide at Midlatitudes With Excess Nitric Oxide at 60°N and S

Latitude	Coefficient
60°N	1.000
55°N	0.979
50°N	0.929
45°N	0.848
40°N	0.763
35°N	0.716
30°N	0.665
30°S	0.551
35°S	0.672
40°S	0.809
45°S	0.894
50°S	0.946
55°S	0.978
60°S	1.000

Table 4. Dates of Geomagnetic Storms and SNOE Observations of Aurorally Produced Nitric Oxide at the Equator

Date of Storm	Ap	Date of SNOE Observation	
4 May 1998	101	5 May 1998	1998/125
27 August 1998	144	28 August 1998	1998/240
25 September 1998	117	26 September 1998	1998/269
15 July 2000	164	17 July 1998	2000/199
12 August 2000	123	13 August 2000	2000/226

[26] A more detailed examination of Figure 6 (bottom) shows that there are individual days when nitric oxide is transported all the way to the equator. Table 4 has a list of the dates of large geomagnetic storms during the 935-day period and the dates of SNOE observations of excess nitric oxide at the equator. The largest value of the Ap index during the storm is also listed.

[27] Using the last column of the table, which lists the day number of the SNOE observation as a guide, a careful examination of Figure 6 (bottom) shows excess nitric oxide extending all the way from the auroral region to the equator on the dates listed in the table. The arrival at the equator has about a 1-day delay compared with the maximum in geomagnetic activity. During some of the storms, the excess nitric oxide remains at the equator for several days. During major geomagnetic storms, the electron precipitation moves equatorward by 5°–10° [*Baker et al.*, 2001]. In Plates 2 and 3 of *Baker et al.* [2001] we show latitude-altitude plots of the behavior of nitric oxide following the 4 May 1998 and 25 September 1998 geomagnetic storms. These figures show the nitric oxide moving equatorward away from the region of electron precipitation. We interpret this behavior as evidence for atmospheric transport. In addition to these five major storms during the 2 1/2 years of observations, there were an additional 14 storms with Ap greater than 50. All of these storms produced enhanced nitric oxide equatorward of the auroral region.

[28] The high correlation of the model calculations and the SNOE observations between 30°S and 30°N is strong confirmation of the hypothesis that solar soft X-rays are the source of the variability of low-latitude nitric oxide [*Barth et al.*, 1988]. The demonstration in this paper that atmospheric winds are transporting nitric oxide equatorward during some seasons suggests that two-dimensional and three-dimensional models be used to properly model the behavior of the nitric oxide. The results in this paper show that it is necessary to properly model the production of photoelectrons and excited nitrogen atoms from the solar soft X-rays in these models to successfully predict the variability of thermospheric nitric oxide.

7. Summary

[29] In the equatorial region of the lower thermosphere (110 km), a time-dependent photochemical model that uses observed values of solar soft X-rays adequately describes the behavior of nitric oxide. In particular, the model properly predicts the changes in the nitric oxide density as a result of daily changes in the solar soft X-ray irradiance in the 2–7 nm wavelength region. The correlation between the observations and the model calculations is high between latitudes 30°S and 30°N.

[30] Electron precipitation in the auroral region, 65° to 75° geomagnetic latitude, is a large and varying source of nitric oxide in the thermosphere. In the lower thermosphere, aurorally produced nitric oxide is transported equatorward by atmospheric transport during the fall-winter season. During large geomagnetic storms, nitric oxide is transported all the way to the equator.

[31] **Acknowledgments.** We thank Mike Stevens for the use of his calculations of the nitric oxide gamma band g-factors. The Student Nitric Oxide Explorer (SNOE) mission was managed for the National Aeronautics and Space Administration by the Universities Space Research Association. The analysis of the SNOE data was sponsored by a grant from NASA Headquarters.

[32] Arthur Richmond thanks the reviewers for their assistance in evaluating this paper.

References

Bailey, S. M., T. N. Woods, C. A. Barth, S. C. Solomon, L. R. Canfield, and R. Korde (2000), Measurements of the solar soft x-ray irradiance by the Student Nitric Oxide Explorer: First analysis and underflight calibrations, *J. Geophys. Res.*, *105*, 27,179–27,193.

Bailey, S. M., C. A. Barth, and S. C. Solomon (2002), A model of nitric oxide in the lower thermosphere, *J. Geophys. Res.*, *107*(A8), 1206, doi:10.1029/2001JA000258.

Baker, D. N., C. A. Barth, K. D. Mankoff, S. G. Bailey, G. M. Mason, and J. E. Mazur (2001), Relationships between precipitating auroral zone electrons and lower thermosphere nitric oxide densities: 1998–2000, *J. Geophys. Res.*, *106*, 24,465–24,480.

Barth, C. A. (1992), Nitric oxide in the lower thermosphere, *Planet. Space Sci.*, *40*, 315–336.

Barth, C. A., W. K. Tobiska, D. E. Siskind, and D. D. Cleary (1988), Solar-terrestrial coupling: Low-latitude thermospheric nitric oxide, *Geophys. Res. Lett.*, *15*, 92–96.

Barth, C. A., K. D. Mankoff, S. M. Bailey, and S. C. Solomon (2003), Global observations of nitric oxide in the thermosphere, *J. Geophys. Res.*, *108*(A1), 1027, doi:10.1029/2002JA009458.

Chamberlain, J. W. (1961), *Physics of the Aurora and Airglow*, Academic, San Diego, Calif.

Colegrove, F. D., W. B. Hanson, and F. S. Johnson (1965), Eddy diffusion and oxygen transport in the lower thermosphere, *J. Geophys. Res.*, *70*, 4931.

Eparvier, F. G., and C. A. Barth (1992), Self-absorption theory applied to rocket measurements of the nitric oxide (1,0) gamma band in the daytime thermosphere, *J. Geophys. Res.*, *97*, 13,723–13,731.

Fuller-Rowell, T. J. (1993), Modeling the solar cycle change in nitric oxide in the thermosphere and upper mesosphere, *J. Geophys. Res.*, *98*, 1559–1570.

Hall, L. A., and G. P. Anderson (1991), High-resolution solar spectrum between 2000 and 3100 A, *J. Geophys. Res.*, *96*, 12,927–12,931.

Hinteregger, H. E., K. Fukui, and G. R. Gilson (1981), Observational, reference, and model data on solar EUV, from measurements on AE-E, *Geophys. Res. Lett.*, *8*, 1147.

Minschwaner, K., and D. E. Siskind (1993), A new calculation of nitric oxide photolysis in the stratosphere, mesosphere, and lower thermosphere, *J. Geophys. Res.*, *98*, 20,401.

Minschwaner, K., J. Bishop, S. A. Budzien, K. F. Dymond, D. E. Siskind, M. H. Stevens, and R. P. McCoy (2004), Middle and upper thermospheric odd nitrogen: 2. Measurements of nitric oxide from ISAAC observations of NO gamma band emission, *J. Geophys. Res.*, *109*, A01304, doi:10.1029/2003JA009941.

Murray, J. E., et al. (1994), Vacuum ultraviolet Fourier transform spectroscopy of the delta (0,0) and beta (7,0) bands of NO, *J. Chem. Phys.*, *101*, 62.

Newell, P. T., K. M. Lyons, and C.-I. Meng (1996), A large survey of electron acceleration events, *J. Geophys. Res.*, *101*, 2599.

Picone, J. M., A. E. Hedin, D. P. Drob, and A. C. Aiken (2002), NRLMSISE-00 empirical model of the atmosphere: Statistical comparisons and scientific issues, *J. Geophys. Res.*, *107*(A12), 1468, doi:10.1029/2002JA009430.

Rottman, G. J., T. N. Woods, and T. P. Sparn (1993), Solar-stellar irradiance comparison experiment, instrument design, and operation, *J. Geophys. Res.*, *98*, 10,667–10,668.

Siskind, D. E. (2000), On the coupling between middle and upper atmosphere odd nitrogen, in *Atmospheric Science Across the Stratosphere*, *Geophys. Monogr. Ser.*, vol. 123, edited by D. E. Siskind, S. D. Eckermann, and M. E. Summers, pp. 101–116, AGU, Washington, D.C.

Siskind, D. E., C. A. Barth, and D. D. Cleary (1990), The possible effect of solar X-rays on thermospheric nitric oxide, *J. Geophys. Res.*, *95*, 4311–4317.

Siskind, D. E., D. J. Strickland, R. R. Meier, T. Majeed, and F. G. Eparvier (1995), On the relationship between the solar soft X-ray flux and thermospheric nitric oxide: An update with an improved photoelectron model, *J. Geophys. Res.*, *100*, 19,687–19,694.

Solomon, S. C., P. B. Hays, and V. J. Abreu (1988), The auroral 6300 A emission: Observations and modeling, *J. Geophys. Res.*, *93*, 9867.

Stevens, M. H. (1995), Nitric oxide gamma band fluorescent scattering and self-absorption: 1. The mesosphere and lower thermosphere, *J. Geophys. Res.*, *100*, 14,735–14,742.

VanHoosier, M. E., J.-D. F. Bartoe, G. E. Brueckner, and D. K. Prinz (1988), Absolute solar spectral irradiance 120 nm–400 nm (results from the Solar Ultraviolet Spectral Irradiance Monitor-SUSIM-experiment on board Spacelab 2), *Astrophys. Lett. Commun.*, *27*, 163–167.

Woods, T. N., et al. (1996), Validation of the UARS solar ultraviolet irradiances: Comparison with the ATLAS 1 and 2 measurements, *J. Geophys. Res.*, *101*, 9541.

S. M. Bailey, Geophysical Institute, University of Alaska, Fairbanks, AK 99775-7320, USA. (scott.bailey@gi.alaska.edu)

C. A. Barth, Laboratory for Atmospheric and Space Physics, University of Colorado, Boulder, CO 80309-0590, USA. (charles.barth@lasp.colorado.edu)